

Published in final edited form as:

J Med Chem. 2008 May 8; 51(9): 2668–2675. doi:10.1021/jm701444y.

Ring size of somatostatin analogues (ODT-8) modulates receptor selectivity and binding affinity

Judit Erchegyi¹, Christy Rani R. Grace², Manoj Samant¹, Renzo Cescato³, Veronique Piccand³, Roland Riek², Jean Claude Reubi³, and Jean E. Rivier^{1,*}

¹The Clayton Foundation Laboratories for Peptide Biology, The Salk Institute for Biological Studies, 10010 N. Torrey Pines Rd., La Jolla, CA 92037, USA ²Structural Biology Laboratory, The Salk Institute for Biological Studies, 10010 N. Torrey Pines Rd., La Jolla, CA 92037, USA ³Division of Cell Biology and Experimental Cancer Research, Institute of Pathology, University of Berne, Berne, Switzerland

Abstract

The synthesis, biological testing and NMR studies of several analogues of H-c[Cys³-Phe⁶-Phe⁷-^DTrp⁸-Lys⁹-Thr¹⁰-Phe¹¹-Cys¹⁴]-OH (ODT-8, a pan-somatostatin analogue) (**1**), have been performed to assess the effect of changing the stereochemistry and the number of the atoms in the disulfide bridge on binding affinity. Cysteine at positions 3 and/or 14 (SRIF numbering) were/was substituted with ^D-cysteine, Nor-cysteine, ^D-Nor-cysteine, Homo-cysteine and/or ^D-Homo-cysteine. The 3D structures of selected partially selective, bioactive analogues (**3**, **18**, **19** and **21**) were carried out in DMSO. Interestingly and not unexpectedly, the 3D structures of these analogues comprised the pharmacophore for which the analogues had the highest binding affinities (i.e., sst₄ in all cases).

Introduction

Somatostatin (SRIF) is a major endocrine hormone with multiple physiological actions¹⁻¹¹ modulated by one or more of the five somatostatin receptors.¹²⁻¹⁶ The biological role, as well as the cellular distribution of each receptor subtype, is far from being completely understood. Availability of receptor subtype-selective ligands is still critical to our understanding of SRIF's physiological role. Numerous analogues are presently being used in the clinic to manage a number of pathophysiological conditions^{4,17-19} and as ligands for radiotherapy.^{20,21}

Constraints, which reduce the flexibility of peptide-backbones or side-chain orientation have been identified, under certain circumstances, to generate analogues with enhanced biological potency, duration of action or selectivity, stability against proteolytic breakdowns, and improved bio-distribution and bioavailability. Such conformational flexibility could allow binding by an induced-fit mechanism and the analogue could exhibit a conformation accommodating two or more pharmacophores simultaneously.

We have shown that the introduction of ^DTrp⁸ in the octapeptide des-AA^{1,2,4,5,12,13}-SRIF^{22,23} resulted in an analogue that binds to all of the five somatostatin receptors (sst_s) similar to SRIF.²⁴ ^DTrp⁸ and IAmP⁹ substitutions in the undecapeptide des-AA^{1,2,5}-SRIF or ^DAgI(NMe, 2naphthoyl)⁸ or *L-threo*-β-MeNal⁸ in the octapeptide des-AA^{1,2,4,5,12,13}-SRIF resulted in a

*Corresponding author: Jean Rivier, The Salk Institute, The Clayton Foundation Laboratories for Peptide Biology, 10010 N. Torrey Pines Road, La Jolla, CA 92037, (858) 453-4100, Fax: (858) 552-1546, jrivier@salk.edu

selective agonist at sst_1 ,²⁵⁻²⁹ a selective antagonist at sst_3 ,^{30,31} and a selective agonist at sst_4 ,^{24,32-34} respectively, by stabilizing the active conformation at these receptors.

The present study describes the synthesis, biological testing, and NMR studies of several analogues of the des-AA^{1,2,4,5,12,13}-[DTrp⁸]-SRIF (ODT-8) (**1**) scaffold. D amino acids and/or unnatural amino acids, which reduce or increase the flexibility of the cyclic backbone, aiming to obtain ligands with high binding affinity at the different receptors and sst-selectivity, were used. We have synthesized a series of ODT-8 analogues in which Cys at positions 3 and/or 14 (SRIF numbering) was substituted with ^DCys, norcysteine (Ncy), ^D-norcysteine (^DNcy),³⁵ homocysteine (Hcy) and ^D-homocysteine (^DHcy). NMR studies of selected analogues identified structural features that may be responsible for binding to more than one receptor.

Results

Peptide Synthesis and Determination of the Stereochemistry of Ncy in the Peptides

All of the analogues shown in Table 1 were synthesized either manually or automatically on a chloromethylated (CM) resin using the Boc-strategy. Boc-Ncy(Mob)-OH, Boc-^D/L-Ncy(Mob)-OH,³⁵ Boc-Hcy(Mob)-OH and Boc-^DHcy(Mob)-OH were synthesized in our laboratory;³⁶ see details in the Experimental section. Peptides containing norcysteine (Ncy) at the N-terminus were unstable during hydrogen fluoride (HF) cleavage/workup conditions and were acetylated by an excess of acetic anhydride in dichloromethane (DCM) on the resin before hydrofluoric acid (HF) cleavage. All of the Ncy-containing Ac-ODT-8 analogues (**9-16**) were synthesized by incorporating racemic Boc-Ncy(Mob)-OH³⁵ or on racemic Boc-Ncy(Mob)-CM resin. The diastereomeric peptides were separated by RP-HPLC and the absolute stereochemistry of Ncy in the Ac-ODT-8 analogues was confirmed by the comparison of the HPLC retention times and coelution of each diastereomer with those of the analogues synthesized separately using resolved Boc-Ncy(Mob)-OH. This approach of determining stereochemistry was successful in analogues containing Ncy residue at position 3 (**9, 10, 15** and **16**) but not in analogues containing Ncy at the C-terminus (**11, 12, 13**, and **14**). Our attempts to link the Boc-Ncy(Mob)-OH in optically active form to the CM resin failed as racemization occurred during the attachment step (2.0 equivalent of KF per mmol of amino acid in DMF at 80 °C for 15 h). It is noteworthy to mention here that optical integrity of the resolved Boc-Ncy(Mob)-OH³⁵ in peptides **9** and **15** was significantly reduced when coupling was mediated under basic conditions (TBTU/DIPEA/HOBt in DMF) instead of neutral conditions (DIC/HOBt in DMF). Hence, to determine the stereochemistry of Ac-ODT-8 analogues containing Ncy (**11 - 14**) at the C-terminus, we used an alternative method²⁸ described by our group for the synthesis of N^α-methylated somatostatin analogues. Based on the premise that failure to attach Boc-Ncy (Mob)-OH in optically active form to the CM resin was due to susceptibility of Ncy residue to racemization under standard coupling conditions, we first synthesized lysine-elongated peptides i.e., [Ncy¹⁴]Ac-ODT-8-Lys and [^DCys³, Ncy¹⁴]Ac-ODT-8-Lys starting with Boc-Lys (2-Cl-Z)-CM resin. The enzymatic hydrolysis of the purified peptides [Ncy¹⁴]Ac-ODT-8-Lys and [^DCys³, Ncy¹⁴]Ac-ODT-8-Lys with a Carboxypeptidase B enzyme preparation³⁷ resulted in the desired non-lysine-containing **11** and **13**, respectively. RP-HPLC studies revealed that **9, 11, 13** and **15** synthesized with the resolved Boc-Ncy(Mob)-OH coeluted with the first eluting diastereomer of the pairs **9 + 10, 11 + 12, 13 + 14**, and **15 + 16**, respectively, on RP-HPLC. Analogues **17-20** were synthesized using racemic Boc-Ncy(Mob)-OH on racemic Boc-Ncy(Mob)-CM resin. The four diastereomers (**17-20**) with retention times of 11.1 min, 12.3 min, 13.1 min and 14.1 min were separated and purified by RP-HPLC. The stereochemistry of the diastereomers **17, 18** and **19** was confirmed by comparison of the HPLC retention times and coelution of each diastereomer with those of the analogues obtained from the enzymatic hydrolysis of lysine-extended peptides [Ncy³, ^DNcy¹⁴]Ac-ODT-8-Lys, [^DNcy³, Ncy¹⁴]Ac-

ODT-8-Lys and [Ncy³, Ncy¹⁴]Ac-ODT-8-Lys, respectively. This confirmed that analogue **20** eluting (*t_R*) at 14.1 min on analytical HPLC contained ^δNcy at positions 3 and 14.

Purification and Characterization of the Analogues (see legend Table 1)

Purification was carried out using multiple HPLC steps.³⁸ Characterization and purity of the analogues were established by HPLC,³⁸ capillary zone electrophoresis³⁹ and mass spectrometry. The C-terminus-extended purified target peptides (RP-HPLC and CZE purity > 96%) could be hydrolyzed with Carboxypeptidase B resulting in the desired analogues. The measured masses obtained by MALDI-MS were within 100 ppm of those calculated for the protonated molecule ions and are given in Table 1.

Receptor binding

The compounds were tested for their ability to bind to the five human sst receptor subtypes (sst₁₋₅) in competitive experiments using ¹²⁵I-[Leu⁸, DTrp²², Tyr²⁵]SRIF-28 as radioligand. Cells stably expressing the five cloned human sst_s were grown as described previously.³ Cell membrane pellets were prepared and receptor autoradiography was performed as previously depicted in detail.³ The binding affinities are expressed as IC₅₀ values that are calculated after quantification of the data using a computer-assisted image processing system as described previously^{3,40} and are summarized in Table 1.

Analogue **1** binds to the five receptors of somatostatin with low nM affinity and has maximum affinity for sst₄. Analogue **2** differs from **1** by a ^δCys at position 3 and binds to all of the somatostatin receptors with higher affinity than analogue **1**. Analogue **3** differs from **1** by a ^δCys at position 14 and does not bind to sst₁. Acetylation of ODT-8 (**1**) results in **5** that binds to all of the sst_s similar to ODT-8 (**1**). The acetylation of **2** and **3** resulting in **6** and **7** has some influence on the binding affinity of these peptides at sst₂ but not at the other sst_s compared with the parent peptides. Analogue **8** differs from **6** having a ^δCys at position 14 and this peptide does not bind to sst₁ but binds to all of the other receptors with similar binding affinity as **6**. Ncy and ^δNcy substitutions at position 3 for Cys in Ac-ODT-8 (**5**) result in **9** and **10** that bind to all sst_s but sst₁ similar to **5**. Analogues **11** and **13** differ from **5** and **6** having Ncy at position 14. Both peptides bind to sst₁ with significantly less affinity than the parent analogues. ^δCys substitution at position 14 has resulted in **15-17** showing enhancement in binding affinity for sst₂ compared to **5**. Similarly, ^δNcy substitution at position 14 resulted in **12, 14, 17** and **20** which bind to sst₂ with higher affinity than **5**. Analogue **18** differs from **1** having ^δNcy at position 3 and Ncy at 14 and has an acetylated N-terminus. It binds to sst₄ in low nM affinity (IC₅₀ = 2.7 nM), and with moderate affinity to receptors sst₂, sst₃ and sst₅, (IC₅₀ = 110 nM, 45 nM and 107 nM, respectively) but does not bind to sst₁. Analogue **19** is similar to **18** except for Ncy residues at position 3. Analogue **19** binds to sst₄ with high affinity (IC₅₀ = 1.6 nM) and shows moderate affinity for receptors sst₂, sst₃ and sst₅, (IC₅₀ = 34 nM, 19 nM and 57 nM, respectively) and weak binding affinity to sst₁ (IC₅₀ = 302 nM). Analogue **21** differs from **1** having Hcy at position 3 and has an acetylated N-terminus. It shows high binding affinity for sst₂ and sst₄ (IC₅₀ = ~ 6 nM and ~ 0.8 nM, respectively) but only moderate affinity for the other three receptors. The substitution of Hcy by ^δHcy in analogue **21** results in analogue **22** that shows lower binding affinity for all of the sst_s than **21**.

To get insights into the action of such non-selective analogues, structural studies in DMSO were carried out despite the fact that the conformation preferred in DMSO may be difficult to interpret since the non-selective analogues may adopt a biologically irrelevant conformation because of their promiscuous properties.

Analogues studied here bind non-selectively to more than one receptor and hence it is interesting to compare their 3D structures in DMSO with the available receptor-selective

pharmacophores.^{29,34,41} Analogues **1**, **3**, **18**, **19** and **21** (Table 1) have been selected for these studies. They have similar structures except for the stereochemistry of the bridgeheads and the number of the atoms involved in the cycle.

NMR Studies

We present details about the chemical shift assignment of proton resonances and structural information for **1**, **3**, **18**, **19** and **21** (Table 1) obtained by solution-state NMR studies in the solvent DMSO.

Assignment of Proton Resonances, Collection of Structural Restraints, and Structure Determination—Almost all chemical shift assignments of proton resonances (Table S2) for all of the analogues (Table 1, assignment and structural characterization of analogue **1** (ODT-8), have been taken from Grace *et al.*³⁴) have been carried out using two-dimensional (2D) NMR experiments applying the standard procedure described in the Experimental section. The N-terminal amino protons for **1** and **3** have not been observed because of fast exchange with the solvent. The N-acetyl terminal amide protons, however, are observed for **18**, **19** and **21**.

A large number of experimental NOEs have been observed for all of the five analogues in the NOESY spectrum measured with a mixing time of 100 ms, leading to over 100 meaningful distance restraints per analogue and concomitantly ~10 restraints per residue (Table 2). These structural restraints were used as input for the structure calculation with the program CYANA⁴² followed by restrained energy minimization using the program DISCOVER.⁴³ The resulting bundle of 20 conformers per analogue represents the 3D structure of each analogue in DMSO. For each analogue, the small residual constraint violations in the distances for the 20 refined conformers (Table 2) and the coincidence of the experimental NOEs and short interatomic distances (data not shown) indicate that the input data represent a self-consistent set, and that the restraints are well satisfied in the calculated conformers (Table 2). The deviations from ideal geometry are minimal, and similar energy values have been obtained for all of the 20 conformers for each analogue. The quality of the structures determined is furthermore reflected by the small backbone RMSD values relative to the mean coordinates of ~0.5 Å (see Table 2 and Figure 2).

Three-dimensional Structure of H-c[Cys³-Phe⁶-Phe⁷-^DTrp⁸-Lys⁹-Thr¹⁰-Phe¹¹-Cys¹⁴]-OH (ODT-8) (1**)**—As we published earlier for analogue **1**³⁴ (Table 1), the backbone torsion angles indicate that a β -turn of type-VIII' conformation is present around Phe⁷-^DTrp⁸. A turn-like structure is also supported by the medium range $d_{\text{NN}}(i,i+2)$ distance restraints (Figure 1). Although the unshifted resonance for the amide proton of Lys⁹ (293-318 K) is indicative of an expected hydrogen bond Lys⁹NH-O⁺Phe⁶, the carbonyl C=O of Phe⁶ is not in a favorable orientation to be involved in a hydrogen bond. The side chain of Phe⁶ is in the *gauche*⁺ rotamer, Phe⁷ is in the *trans* rotamer, ^DTrp⁸ is in the *gauche*⁻ rotamer and Lys⁹ is in the *gauche*⁺ rotamer (Table S1). Conclusively, the side chains of ^DTrp⁸ and Phe⁷ are adjacent to each other in the plane of the analogue backbone, whereas the side chains of Phe⁶ and Phe¹¹ are pointing away from the plane of the peptide backbone.³⁴

Three-dimensional Structure of H-c[Cys³-Phe⁶-Phe⁷-^DTrp⁸-Lys⁹-Thr¹⁰-Phe¹¹-^DCys¹⁴]-OH (3**)**—For analogue **3** (Table 1), the backbone torsion angles do not fit into any of the classified reported β -turns in literature. The side chains of Phe⁶, Phe⁷, ^DTrp⁸, Lys⁹ and Phe¹¹ are in the *gauche*⁺ rotamer (Table S1). This configuration orients Phe⁷, Phe¹¹ and Lys⁹ pointing away from the backbone on one side, while the side chains of Phe⁶ and ^DTrp⁸ point on the opposite side (Figure 2). Ring current of Phe¹¹ resulted in slightly upfield shifted resonances for the γ -protons of Lys⁹ (Table S2).

Three-dimensional Structure of Ac-c[^DNcy³-Phe⁶-Phe⁷-^DTrp⁸-Lys⁹-Thr¹⁰-Phe¹¹-Ncy¹⁴]-OH (18)—For analogue **18** (Table 1), the backbone torsion angles indicate a β -turn of type-II conformation around Phe⁷-^DTrp⁸ (Table S1). The side chain of Phe⁶, ^DTrp⁸, Lys⁹ are in the *gauche*⁺ rotamer, Phe⁷ is in the *trans* rotamer and Phe¹¹ is in the *gauche*⁻ rotamer (Table S1). Hence, the side chains of Phe⁷ and ^DTrp⁸ adjacent to each other are in the plane of the peptide backbone, while the side chains of Lys⁹ and Phe⁶ are in close proximity. The side chain of Phe¹¹ is far away from the ^DTrp-Lys pair behind the peptide backbone (Figure 2). Ring current of Phe⁶ has resulted in slightly up field-shifted resonance for the γ -protons of Lys⁹. Hydrogen bonds are observed in all of the calculated twenty conformers between the amide protons of Lys⁹, Thr¹⁰ and the carbonyl of Phe⁶ and also between the amide proton of Phe⁶ and the carbonyl of Thr¹⁰. Experimentally measured small temperature coefficients of -0.02, -0.004 and -0.01 ppm/K for the amide protons of Phe⁶, Lys⁹ and Thr¹⁰, respectively, confirms that these amide protons are involved in the hydrogen bond.

Three-dimensional Structure of Ac-c[Ncy³-Phe⁶-Phe⁷-^DTrp⁸-Lys⁹-Thr¹⁰-Phe¹¹-Ncy¹⁴]-OH (19)—For analogue **19** (Table 1), the backbone torsion angles do not fit into any of the classified β -turns reported in the literature. The side chains of Phe⁶, Phe⁷, ^DTrp⁸, Lys⁹ and Phe¹¹ are in the *gauche*⁺ rotamer (Table S1). This orients the side chain of Phe⁶, Lys⁹ and Phe¹¹ on one side of the peptide backbone, with Phe¹¹ in close proximity to Lys⁹. Side chains of Phe⁷ and ^DTrp⁸ are in the plane of the peptide backbone (Figure 2).

Three-dimensional Structure of Ac-c[Hcy³-Phe⁶-Phe⁷-^DTrp⁸-Lys⁹-Thr¹⁰-Phe¹¹-Cys¹⁴]-OH (21)—The backbone torsion angles from the 3D structures show that an inverse γ -turn is present around ^DTrp⁸ for analogue **21** (Table 1). The side chains of Phe⁶, Phe⁷, Lys⁹ and Phe¹¹ are in *gauche*⁺ rotamer and that of ^DTrp⁸ is in *gauche*⁻ rotamer (Table S1). This orients the side chains of Phe⁶, Phe⁷ and Lys⁹ on one side of the peptide backbone, while the side chains of ^DTrp⁸ and Phe¹¹ are on the other side (Figure 2). Close proximity between the amide group of Lys⁹ and the carbonyl of Phe⁷, as well as the amide group of Thr¹⁰ and the carbonyl of the acetyl group at the N-terminus shows possible hydrogen bonds between these groups. Experimentally measured small temperature coefficients of -0.01, -0.002 ppm/K for the amide protons of Phe⁷ and Thr¹⁰, respectively, confirm that these amide protons are involved in a hydrogen bond.

Discussion

All of the five analogues studied here by NMR in DMSO bind non-selectively to more than one receptor and hence it is interesting to compare their structures with receptor-selective pharmacophores. However, because of the non-selective binding of these analogues, the elucidation of such a multiple structure-activity relationship is not trivial and a step-by-step analysis is required. Therefore, we first review the structural parameters proposed for the receptor-selective pharmacophores^{29,34,41,44} followed by a discussion of the 3D structures of the non-selective analogues of interest.

Pharmacophores of Somatostatin Receptors

Receptor-selective agonistic analogues binding selectively to somatostatin receptors 1, 2, and 4 have been obtained by using both chemical modifications of different amino acid side chain groups in short SRIF analogues,^{26,45} as well as structural design to optimize the pharmacophore.^{29,34,41} The pharmacophore for sst₁ binding has been shown to be the ^DTrp⁸-IAmp⁹ (4-(N-isopropyl)-aminomethylphenylalanine) pair of residues in addition to two aromatic side chains at position 7 and 11.²⁹ Based on the pharmacophore and other experimental findings,^{25,46} the rationale is that the longer side chain of IAmp can only be accommodated by somatostatin receptor 1, whereas in the other somatostatin receptors, the

binding cavity is limited to accommodating a smaller side chain as that of Lys. In contrast to the role of the IAmP in receptor-selectivity, the two aromatic side chains at position 7 and 11 are important to enhance the binding to sst₁ (Figure 3A).

Design of an sst₄-selective agonist was more straightforward.³² The 3D structures of several sst₄-selective analogues identified the pharmacophore for sst₄ to have one aromatic ring of Phe at position 6 or 11 close to Lys⁹, in addition to the crucial ^oTrp⁸ and Lys⁹ pair³⁴ (Figure 3D). The development of a strictly sst₂-selective analogue appears to be more demanding since analogues binding with nM affinity to somatostatin receptor 2 often also bind with high affinity to somatostatin receptor 5 and sometimes to receptor 3.^{47,48} Most of these partially selective analogues are based on the structure of an SRIF analog named octreotide and have a type-II' β -turn in their structure.⁴⁴ The octreotide pharmacophore requires two aromatic side chains at position 7 and 2 in addition to the ^oTrp⁸-Lys⁹ pair. It has also been shown that octreotide-type analogues undergo conformational change in their backbone from β -sheet to α -helix resulting in two different positions for the Phe/^oPhe/Tyr at position 2.⁴⁷ This conformational exchange complicates the basis for receptor-selectivity and suggests that two conformations are necessary for an analogue to fit into the two different receptor-selective pharmacophores for receptors 2 and 5 (Figure 3C). Recently, we published data showing that removal of the aromatic side chain at position 7 from an octreotide analogue led to sst₂-selectivity.⁴¹ Hence, the pharmacophore of an sst₂-selective agonist indeed appears to be a subset of the octreotide pharmacophore with one aromatic side chain of Phe² in addition to the side chains of the ^oTrp⁸ - Lys⁹ pair. Furthermore, in contrast to octreotide, where Phe² undergoes conformational exchange, the sst₂-selective pharmacophore has Phe² at a single position (Figure 3B).

Although sst₃-selective agonists have not been reported yet, there is a report on sst₃-selective antagonists, which have aminoglycine (Agl) at position 8³⁰ instead of Trp/^oTrp and the structure of this analogue has been reported in water.³¹ Similarly, SRIF agonists or antagonists selectively binding to sst₅ have not been described. In summary, selective binding to a receptor requires a unique pharmacophore for the analogues, having Trp⁸, Lys⁹ (or an amino acid with a different side chain) and a specific number of aromatic residues at the correct distances with respect to each other (Figure 3, Table 3).

Comparison of the 3D Structures of Non-Selective Somatostatin Analogues with Receptor-Selective Pharmacophores

Since shortening or lengthening the side chains of Cys at position 3 and 14 of Ac-ODT-8 have resulted in loss of binding to some receptors, we decided to compare the 3D structures of these non-selective analogues in DMSO to that of the corresponding receptor-selective pharmacophores determined earlier.^{29,34,41} All structural data reported above support the fact that the backbone conformation is not responsible in the binding of peptides, rather it acts as a scaffold in orienting the side chains of the analogues to interact efficiently with the receptor. Such conclusions had also been derived based on the NMR structure of astressin (a corticotropin releasing factor antagonist) in DMSO or when bound to the ECD1 of CRF-R2.⁴⁹⁻⁵¹

Hence, the spatial orientation of the amino acid side chains for the different analogues are compared here with that of the receptor-selective pharmacophores. To explain the non-selective binding of an analogue to multiple receptors, either conformational flexibility is necessary to allow binding by an induced-fit mechanism or the analogue prefers a conformation accommodating two or more pharmacophores simultaneously. In particular, the conformation preferred by non-selective analogues in DMSO will not evidently fit all of the pharmacophores simultaneously as proposed.

Comparison of the 3D Structures of the Non-Selective Analogues with the Sst₁-selective Pharmacophore

A comparison of the 3D structures of the non-selective analogues with the sst₁-selective pharmacophore shows the following: The introduction of Ncy in the ODT-8 structure (i.e., in **3**, **18** and **19**) has resulted in loss of binding to receptor 1. Their 3D structures determined in DMSO show that of the three aromatic residues, two of them are oriented on the front side of the peptide backbone. Since the sst₁ pharmacophore requires two aromatic side chains at the backside of the peptide backbone in addition to Trp⁸ and Lys⁹ side chains as shown in Figure 3A²⁹ and Table 3, the sst₁ pharmacophore is not observed in **3**, **18** and **19**. This may explain why **3**, **18** and **19** do not bind to receptor 1. In contrast, the 3D structure of ODT-8 (**1**), which binds to all of the five receptors, has the sst₁ pharmacophore as well.

Comparison of the 3D Structures of the Non-Selective Analogues with the Sst_{2,4}-Selective Pharmacophores

The sst₂-selective pharmacophore requires one aromatic side chain far from the Trp⁸-Lys⁹ pair in addition to these two side chains as shown in Figure 3B⁴¹ and Table 3. Although **1**, **3**, **18**, **19** and **21** bind to receptor 2 with nM affinity, the 3D NMR structures of the analogues in DMSO show that these analogues do not have the sst₂ selective pharmacophore (Figure 4). In **1**, **18** and **21**, a small conformational change of the side chain of either Phe⁶ or Phe¹¹ can establish the partially selective pharmacophore (Figure 4). But in **3** and **19**, the side chain of Phe⁶ has to undergo a large conformational change to fit the sst₂-selective pharmacophore. Therefore, the 3D structures of the analogues determined in DMSO are not sufficient to explain the sst_{2,5} non-selective pharmacophore.

Also ⁿCys or ⁿNcy substitution at position 14 has resulted in analogues (**3**, **4**, **7**, **8**, **15**, **16** or **12**, **14**, **17** and **20**) showing enhanced binding affinity for sst₂ compared to **5**. A D-amino acid, part of the cycle at the C-terminus, changes the backbone conformation, probably bringing the side chains of Phe¹¹ close to the sst₂ pharmacophore (Figure 4). In addition, all of these analogues do not bind to sst₁, probably due to the positioning of the side chain of Phe¹¹, critical for sst₁ binding (Figure 3A).

However, these analogues have the highest affinity for receptor 4 and the sst₄ pharmacophore is present in their conformations. The sst₄-selective pharmacophore requires one aromatic side chain close to Lys⁹ in addition to side chains of Trp⁸ and Lys⁹ as shown in Figure 3C. The distances between the C_γ atoms of the side chains to fit the sst₄ pharmacophore are given in Table 3. The 3D structures of **1**, **3**, **18**, **19** and **21** have the sst₄ pharmacophore as shown in Figure 5, with either Phe¹¹ (**1**, **3** and **19**) or Phe⁶ (**18** and **21**), involved in sst₄ binding in addition to the necessary ⁿTrp⁸ and Lys⁹ side chains.

Conclusions

Synthesis, binding and 3D NMR structure of non-selective analogues of H-c(Cys-Phe-Phe-DTrp-Lys-Thr-Phe-Cys)-OH (ODT-8, **1**) containing different side chain lengths for the Cys at position 3 and 14 have been presented here. These analogues bind non-selectively to all of the five SRIF receptors and the elucidation of a structure-activity relationship is challenging. In our attempt to establish such a relationship between the 3D structures of the analogues determined in DMSO and their receptor-specificity, it has been observed that the 3D structures mostly have the pharmacophore for which the analogues have the highest binding affinities. All of these analogues bind to sst₄ with the highest binding affinity and their 3D structures have the sst₄ pharmacophore. However, the pharmacophores of the other receptors are often not covered by the 3D structure determined in DMSO and their pharmacophores can only be established by reorientation of some of the amino acid side chains.

The establishment of receptor-selective and non-selective analogues of somatostatin by introducing small chemical modifications to the peptides highlights the complexity of a binding event. The structure determination of these analogues in DMSO elucidates thereby at least in part, the nature of this complexity.

EXPERIMENTAL PROCEDURES

Determination of the stereochemistry of Ncy¹⁴ in the analogues

The fully protected Ac-Ncy(Mob)³-Phe⁶-Phe⁷-^DTrp⁸-Lys(2-Cl-Z)⁹-Thr(Bzl)¹⁰-Phe¹¹-Ncy(Mob)¹⁴-Lys(2-Cl-Z)¹⁵-CM resin (SRIF numbering) was synthesized, cleaved from the resin by HF and purified on preparative RP-HPLC. The purified peptide Ac-Ncy³-Phe⁶-Phe⁷-^DTrp⁸-Lys⁹-Thr¹⁰-Phe¹¹-Ncy¹⁴-Lys¹⁵-OH (20 mg, 16.30 μM) was hydrolyzed in 0.1M NaCl-0.05M Tris buffer at pH 7.6 (20 mL) with undiluted Carboxypeptidase B enzyme solution (50 U) at room temperature. The hydrolysis was complete in 30 min resulting in analogue **19** (Table 1). The product was desalted by preparative RP-HPLC and pure peptide **19** (12 mg, 10.9 μM) was obtained (yield of hydrolysis: 66.87%). Analogues **11**, **13**, **17** and **18** were obtained from the lysine-extended peptides [Ncy¹⁴]Ac-ODT-8-Lys, [^DCys³, Ncy¹⁴]Ac-ODT-8-Lys, [Ncy³, ^DNcy¹⁴]Ac-ODT-8-Lys and [^DNcy³, Ncy¹⁴]Ac-ODT-8-Lys, respectively, in comparable yield using this protocol.

Cell culture

CHO-K1 cells stably expressing human sst₁ and sst₅ were kindly provided by Drs. T. Reisine and G. Singh (University of Pennsylvania, Philadelphia, PA) and CCL39 cells stably expressing human sst₁, sst₂, sst₃, and sst₄ by Dr. D. Hoyer (Novartis Pharma, Basel, Switzerland). Cells were grown as described previously.³ All culture reagents were supplied by Gibco BRL, Life Technologies (Grand Island, NY).

Receptor binding

Cell membrane pellets were prepared and receptor autoradiography was performed as depicted in detail previously.³ Binding studies were performed as reported previously³ with [Leu⁸,^DTrp²², ¹²⁵I Tyr²⁵]-SRIF-28 on cell pellet sections and on tissue sections of the respective sst-expressing human tumors using 15,000 cpm/100 μL of the radioligand.

Sample preparation and NMR experiments

NMR samples were prepared by dissolving 2 mg of the analogue in 0.5 mL of DMSO-d₆. The ¹H NMR spectra were recorded on a Bruker 700 MHz spectrometer operating at proton frequency of 700 MHz as reported previously.^{29,34,41,49,50,52}

Structure Determination

The chemical shift assignment of the major conformer (the population of the minor conformer was <10%) was obtained by the standard procedure using DQF-COSY and TOCSY spectra for intra-residual assignment and the NOESY spectrum was used for the sequential assignment.⁵³ The collection of structural restraints was based on the NOEs assigned manually and vicinal ³J_{NHα} couplings. Dihedral angle constraints were obtained from the ³J_{NHα} couplings, which were measured from the 1D ¹H NMR spectra and from the intra-residual and sequential NOEs along with the macro GRIDSEARCH in the program CYANA.⁴² The calibration of NOE intensities versus ¹H-¹H distance restraints and appropriate pseudo-atom corrections to the non-stereo specifically assigned methylene, methyl and ring protons were performed using the program CYANA. On an average, approximately 100 NOE constraints and 20 angle constraints were utilized while calculating the conformers (Table 2). A total of 100 conformers were initially generated by CYANA and a bundle containing 20 CYANA conformers with the

lowest target function values were utilized for further restrained energy minimization, using the CFF91 force field⁵⁴ with the energy criteria fit 0.1 kcal/mol/Å⁵⁵ in the program DISCOVER with steepest decent and conjugate gradient algorithms.⁵⁶ The resulting energy minimized bundle of 20 conformers was used as a basis for discussing the solution conformation of the different SRIF analogues. The structures were analyzed using the program MOLMOL.⁵⁷

Supplementary Material

Refer to Web version on PubMed Central for supplementary material.

Acknowledgments

This work was supported in part by NIH grant R01 DK059953. We are indebted to R. Kaiser and C. Miller for technical assistance in the characterization of the peptides, Dr. W. Fisher, and W. Low for mass spectrometric analysis of the analogues and D. Doan for manuscript preparation. JR is the Dr. Frederik Paulsen Chair in Neurosciences Professor.

Abbreviations

The abbreviations for the common amino acids are in accordance with the recommendations of the IUPAC-IUB Joint Commission on Biochemical Nomenclature (Eur. J. Biochem. 1984, 138:9-37). The symbols represent the L-isomer except when indicated otherwise. Additional abbreviations:

Boc	t-Butoxycarbonyl
Bzl	benzyl
Z(2Cl)	2-chlorobenzyloxycarbonyl
CZE	capillary zone electrophoresis
CYANA	Combined assignment and dynamics algorithm for NMR applications
DIC	N,N'-diisopropylcarbodiimide
DIPEA	diisopropylethylamine
DMF	dimethylformamide
DMSO	dimethylsulfoxide
DQF-COSY	double quantum filtered correlation spectroscopy
Hcy	homocysteine
HOBt	1-hydroxybenzotriazole
IAMP	4-(N-isopropyl)-aminomethylphenylalanine
IBMX	3-isobutyl-1-methylxanthine
Mob	4-methoxybenzyl
Ncy	norcysteine
NMR	nuclear magnetic resonance
NOESY	nuclear Overhauser enhancement spectroscopy

3D	three-dimensional
OBzl	benzyl ester
PROSA	Processing algorithms
RMSD	root mean square deviation
SAR	structure activity relationships
SRIF	somatostatin
sst₅	SRIF receptors
TEA	triethylamine
TEAP	triethylammonium phosphate
TFA	trifluoroacetic acid
TOCSY	total correlation spectroscopy

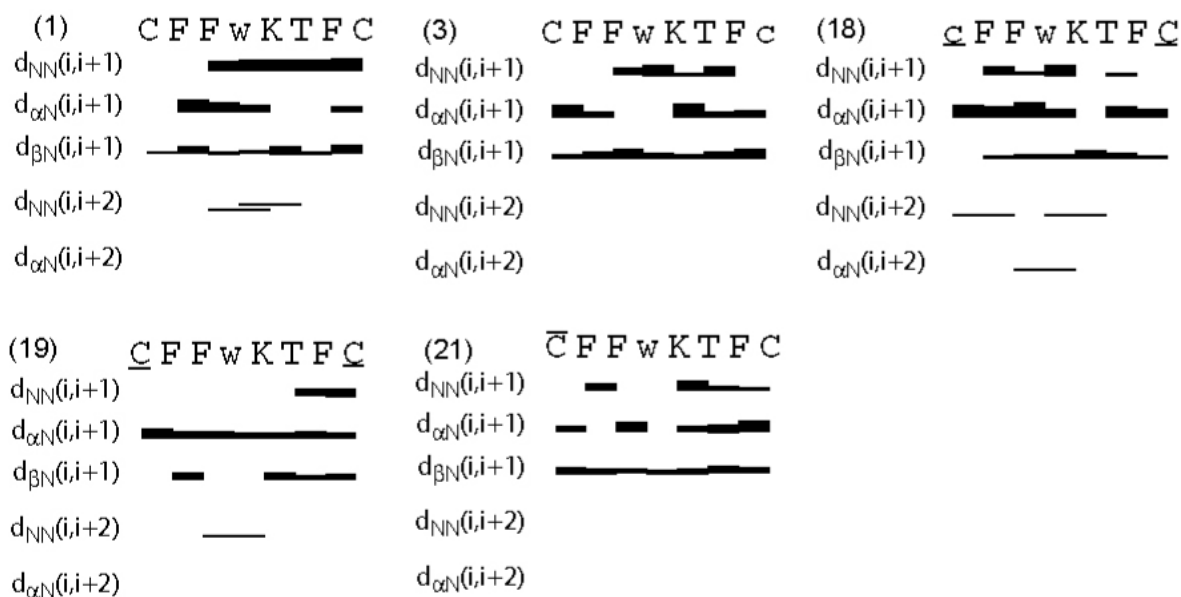
References

- (1). Brazeau P, Vale W, Burgus R, Ling N, Butcher M, Rivier J, Guillemin R. Hypothalamic polypeptide that inhibits the secretion of immunoreactive pituitary growth hormone. *Science* 1973;179:77–79. [PubMed: 4682131]
- (2). Guillemin R, Gerich JE. Somatostatin: physiological and clinical significance. *Ann. Rev. Med* 1976;27:379–388. [PubMed: 779605]
- (3). Reubi JC, Schaer JC, Waser B, Wenger S, Heppeler A, Schmitt JS, Mäcke HR. Affinity profiles for human somatostatin receptor sst1–sst5 of somatostatin radiotracers selected for scintigraphic and radiotherapeutic use. *Eur. J. Nucl. Med* 2000;27:273–282. [PubMed: 10774879]
- (4). Janecka A, Zubrzycka M, Janecki T. Review: Somatostatin analogs. *J. Pept. Res* 2001;58:91–107. [PubMed: 11532069]
- (5). Schally AV, Comaru-Schally AM, Nagy A, Kovacs M, Szepeshazi K, Plonowski A, Varga JL, Halmos G. Hypothalamic hormones and cancer. *Front. Neuroendocrinol* 2001;22:248–291. [PubMed: 11587553]
- (6). Lamberts SW, van der Lely AJ, Hofland LJ. New somatostatin analogs: will they fulfil old promises? *Eur. J. Endocrinol* 2002;146:701–705. [PubMed: 11980627]
- (7). Weckbecker G, Lewis I, Albert R, Schmid HA, Hoyer D, Bruns C. Opportunities in somatostatin research: biological, chemical and therapeutic aspects. *Nat. Rev. Drug Discov* 2003;2:999–1017. [PubMed: 14654798]
- (8). van der Hoek J, Hofland LJ, Lamberts SW. Novel subtype specific and universal somatostatin analogues: clinical potential and pitfalls. *Curr. Pharm. Des* 2005;11:1573–1592. [PubMed: 15892663]
- (9). Reubi JC. Peptide receptors as molecular targets for cancer diagnosis and therapy. *Endocr. Rev* 2003;24:389–427. [PubMed: 12920149]
- (10). Panteris V, Karamanolis DG. The puzzle of somatostatin: action, receptors, analogues and therapy. *Hepatogastroenterology* 2005;52:1771–1781. [PubMed: 16334776]
- (11). Petersenn S. Efficacy and limits of somatostatin analogs. *J. Endocrinol. Invest* 2005;28:53–57. [PubMed: 16625846]
- (12). Tulipano G, Schulz S. Novel insights in somatostatin receptor physiology. *Eur. J. Endocrinol* 2007;156(Suppl 1):S3–S11. [PubMed: 17413186]
- (13). Reisine T, Bell GI. Molecular biology of somatostatin receptors. *Endocrine Rev* 1995;16:427–442. [PubMed: 8521788]
- (14). Csaba Z, Dournaud P. Cellular biology of somatostatin receptors. *Neuropeptides* 2001;35:1–23. [PubMed: 11346306]

- (15). Moller LN, Stidsen CE, Hartmann B, Holst JJ. Somatostatin receptors. *Biochim. Biophys. Acta* 2003;1616:1–84. [PubMed: 14507421]
- (16). Olias G, Viollet C, Kusserow H, Epelbaum J, Meyerhof W. Regulation and function of somatostatin receptors. *J. Neurochem* 2004;89:1057–1091. [PubMed: 15147500]
- (17). Reubi JC, Waser B, Liu Q, Laissue JA, Schonbrunn A. Subcellular distribution of somatostatin sst2A receptors in human tumors of the nervous and neuroendocrine systems: Membranous *versus* intracellular location. *J. Clin. Endocrinol. Metab* 2000;85:3882–3891. [PubMed: 11061553]
- (18). Lewis I, Bauer W, Albert R, Chandramouli N, Pless J, Weckbecker G, Bruns C. A novel somatostatin mimic with broad somatotropin release inhibitory factor receptor binding and superior therapeutic potential. *J. Med. Chem* 2003;46:2334–2344. [PubMed: 12773038]
- (19). Reubi JC, Waser B, Schaer J-C, Laissue JA. Somatostatin receptor sst1-sst5 expression in normal and neoplastic human tissues using receptor autoradiography with subtype-selective ligands. *Eur. J. Nucl. Med* 2001;28:836–846. [PubMed: 11504080]
- (20). Reubi JC, Macke HR, Krenning EP. Candidates for Peptide receptor radiotherapy today and in the future. *J. Nucl. Med* 2005;46:67S–75S. [PubMed: 15653654]
- (21). Eberle AN, Mild G, Froidevaux S. Receptor-mediated tumor targeting with radiopeptides. Part 1. General concepts and methods: applications to somatostatin receptor-expressing tumors. *J. Recept. Signal Transduct. Res* 2004;24:319–455. [PubMed: 15648449]
- (22). Vale, W.; Rivier, C.; Brown, M.; Rivier, J. *Hypothalamic Peptide Hormones and Pituitary Regulation: Advances in Experimental Medicine and Biology*. Plenum Press; New York: 1977. Pharmacology of TRF, LRF and somatostatin; p. 123-156.
- (23). Vale W, Rivier J, Ling N, Brown M. Biologic and immunologic activities and applications of somatostatin analogs. *Metabolism* 1978;27:1391–1401. [PubMed: 210361]
- (24). Rivier J, Erchegyi J, Hoeger C, Miller C, Low W, Wenger S, Waser B, Schaer J-C, Reubi JC. Novel sst4-selective somatostatin (SRIF) agonists. Part I: Lead identification using a betide scan. *J. Med. Chem* 2003;46:5579–5586. [PubMed: 14667212]
- (25). Chen L, Hoeger C, Rivier J, Fitzpatrick VD, Vandlen RL, Tashjian AH Jr. Structural basis for the binding specificity of a SSTR1-selective analog of somatostatin. *Biochem. Biophys. Res. Commun* 1999;258:689–694. [PubMed: 10329447]
- (26). Rivier JE, Hoeger C, Erchegyi J, Gulyas J, DeBoard R, Craig AG, Koerber SC, Wenger S, Waser B, Schaer J-C, Reubi JC. Potent somatostatin undecapeptide agonists selective for somatostatin receptor 1 (sst1). *J. Med. Chem* 2001;44:2238–2246. [PubMed: 11405660]
- (27). Rivier JE, Kirby DA, Erchegyi J, Waser B, Eltschinger V, Cescato R, Reubi JC. Somatostatin receptor 1 selective analogues: 3. Dicyclic peptides. *J. Med. Chem* 2005;48:515–522. [PubMed: 15658865]
- (28). Erchegyi J, Hoeger CA, Low W, Hoyer D, Waser B, Eltschinger V, Schaer J-C, Cescato R, Reubi JC, Rivier JE. Somatostatin receptor 1 selective analogues: 2. N-methylated scan. *J. Med. Chem* 2005;48:507–514. [PubMed: 15658864]
- (29). Grace CRR, Durrer L, Koerber SC, Erchegyi J, Reubi JC, Rivier JE, Riek R. Somatostatin receptor 1 selective analogues: 4. Three-dimensional consensus structure by NMR. *J. Med. Chem* 2005;48:523–533. [PubMed: 15658866]
- (30). Reubi JC, Schaer J-C, Wenger S, Hoeger C, Erchegyi J, Waser B, Rivier J. SST3-selective potent peptidic somatostatin receptor antagonists. *Proc. Natl. Acad. Sci. USA* 2000;97:13973–13978. [PubMed: 11095748]
- (31). Gairi M, Saiz P, Madurga S, Roig X, Erchegyi J, Koerber SC, Reubi JC, Rivier JE, Giralt E. Conformational analysis of a potent SSTR3-selective somatostatin analogue by NMR in water solution. *J. Peptide Sci* 2006;12:82–91. [PubMed: 16365912]
- (32). Erchegyi J, Penke B, Simon L, Michaelson S, Wenger S, Waser B, Cescato R, Schaer J-C, Reubi JC, Rivier J. Novel sst4-selective somatostatin (SRIF) agonists. Part II: Analogues with β -methyl-3-(2-naphthyl)-alanine substitutions at position 8. *J. Med. Chem* 2003;46:5587–5596. [PubMed: 14667213]
- (33). Erchegyi J, Waser B, Schaer J-C, Cescato R, Brazeau JF, Rivier J, Reubi JC. Novel sst4-selective somatostatin (SRIF) agonists. Part III: Analogues amenable to radiolabeling. *J. Med. Chem* 2003;46:5597–5605. [PubMed: 14667214]

- (34). Grace CRR, Erchegyi J, Koerber SC, Reubi JC, Rivier J, Riek R. Novel sst₄-selective somatostatin (SRIF) agonists. Part IV: Three-dimensional consensus structure by NMR. *J. Med. Chem* 2003;46:5606–5618. [PubMed: 14667215]
- (35). Samant MP, Rivier JE. Norcystine, a new tool for the study of the structure-activity relationship of peptides. *Org. Lett* 2006;8:2361–2364. [PubMed: 16706526]
- (36). Armstrong MD, Lewis JD. Thioether derivatives of cysteine and homocysteine. *J. Org. Chem* 1950;16:749–753.
- (37). Ambler, RP. *Methods in Enzymology*. Academic Press; New York: 1967. p. 437
- (38). Miller C, Rivier J. Peptide chemistry: Development of high-performance liquid chromatography and capillary zone electrophoresis. *Biopolymers Pept. Sci* 1996;40:265–317.
- (39). Miller C, Rivier J. Analysis of synthetic peptides by capillary zone electrophoresis in organic/aqueous buffers. *J. Pept. Res* 1998;51:444–451. [PubMed: 9650719]
- (40). Reubi JC, Schaer JC, Waser B, Hoeger C, Rivier J. A selective analog for the somatostatin sst1-receptor subtype expressed by human tumors. *Eur. J. Pharmacol* 1998;345:103–110. [PubMed: 9593601]
- (41). Grace CRR, Erchegyi J, Koerber SC, Reubi JC, Rivier J, Riek R. Novel sst₂-selective somatostatin agonists. Three-dimensional consensus structure by NMR. *J. Med. Chem* 2006;49:4487–4496. [PubMed: 16854054]
- (42). Güntert P, Mumenthaler C, Wüthrich K. Torsion angle dynamics for NMR structure calculation with the new program DYANA. *J. Mol. Biol* 1997;273:283–298. [PubMed: 9367762]
- (43). Hagler AT, Dauber P, Osguthorpe DJ, Hempel JC. Dynamics and conformational energetics of a peptide hormone: vasopressin. *Science* 1985;227:1309–1315. [PubMed: 3975616]
- (44). Melacini G, Zhu Q, Osapay G, Goodman M. A refined model for the somatostatin pharmacophore: Conformational analysis of lanthionine-sandostatin analogs. *J. Med. Chem* 1997;40:2252–2258. [PubMed: 9216844]
- (45). Erchegyi, J.; Hoeger, C.; Wenger, S.; Waser, B.; Schaer, J-C.; Reubi, J.C.; Rivier, J.E. N-methyl scan of a sst1-selective somatostatin (SRIF) analog; Peptides - The wave of the future: 2nd International Peptide Symposium/17th American Peptide Symposium; American Peptide Symposium: San Diego, CA, 2001; p. 719-720.
- (46). Liapakis G, Fitzpatrick D, Hoeger C, Rivier J, Vandlen R, Reisine T. Identification of ligand binding determinants in the somatostatin receptor subtypes mSSTR1 and mSSTR2. *J. Biol. Chem* 1996;271:20331–20339. [PubMed: 8702767]
- (47). Melacini G, Zhu Q, Goodman M. Multiconformational NMR analysis of sandostatin (octreotide): Equilibrium between β -sheet and partially helical structures. *Biochemistry* 1997;36:1233–1241. [PubMed: 9063871]
- (48). Osapay G, Prokai L, Kin H-S, Medzihradsky KF, Coy DH, Liapakis G, Reisine T, Melacini G, Zhu Q, Wang SH-H, Mattern R-H, Goodman M. Lanthionine-somatostatin analogs: Synthesis, characterization, biological activity, and enzymatic stability studies. *J. Med. Chem* 1997;40:2241–2251. [PubMed: 9216843]
- (49). Grace CRR, Perrin M, DiGruccio M, Miller C, Rivier J, Vale W, Riek R. NMR structure and peptide hormone binding site of the first extracellular domain of a type B1 G-protein coupled receptor. *Proc. Natl. Acad. Sci. USA* 2004;101:12836–12841. [PubMed: 15326300]
- (50). Grace CRR, Perrin M, Gulyas J, DiGruccio M, Cattle JP, Rivier J, Vale W, Riek R. Structure of the N-terminal domain of a type B1 G-protein coupled receptor in complex with a peptide ligand. *Proc. Natl. Acad. Sci. USA* 2007;104:4858–4863. [PubMed: 17360332]
- (51). Horiki K, Igano K, Inouye K. Amino acids and peptides. Part 6. Synthesis of the Merrifield resin esters of N-protected amino acids with the aid of hydrogen bonding. *Chem. Lett* 1978;2:165–168.
- (52). Grace CRR, Cervini L, Gulyas J, Rivier J, Riek R. Astressin-amide and astressin-acid are structurally different in DMSO. *Biopolymers* 2007;87:196–205. [PubMed: 17657708]
- (53). Wüthrich, K. *NMR of Proteins and Nucleic Acids*. J. Wiley & Sons; New York: 1986.
- (54). Maple JR, Thacher TS, Dinur U, Hagler AT. Biosym force field research results in new techniques for the extraction of inter- and intramolecular forces. *Chem. Design Auto. News* 1990;5:5–10.

- (55). Koerber SC, Rizo J, Struthers RS, Rivier JE. Consensus bioactive conformation of cyclic GnRH antagonists defined by NMR and molecular modeling. *J. Med. Chem* 2000;43:819–828. [PubMed: 10715150]
- (56). Hagler, AT. *The Peptides: Analysis, Synthesis, Biology*. Academic Press; Orlando, FL: 1985. Theoretical simulation of conformation, energetics and dynamics of peptides; p. 213-299.
- (57). Koradi R, Billeter M. MOLMOL: a program for display and analysis of macromolecular structures. *PDB Newsletter* 1998;84:5–7.

**Figure 1.**

Survey of characteristic NOEs describing the secondary structure of the five analogues studied by NMR (i.e., analogues **1**, **3**, **18**, **19** and **21** as indicated). Thin, medium and thick bars represent weak (4.5 to 6 Å), medium (3 to 4.5 Å) and strong (< 3 Å) NOEs observed in the NOESY spectrum. The medium-range connectivities $d_{NN}(i,i+2)$, $d_{\alpha N}(i,i+2)$, and $d_{\beta N}(i,i+2)$ are shown by lines starting and ending at the positions of the residues related by the NOE. Residues Ncy, ^DNcy, Hcy, ^DHcy, ^DCys, ^DTrp refer to norcysteine, ^D-norcysteine, homocysteine, ^D-homocysteine, ^D-cysteine and ^D-tryptophan denoted by the symbols, C, c, \bar{C} , \bar{c} and w, respectively.

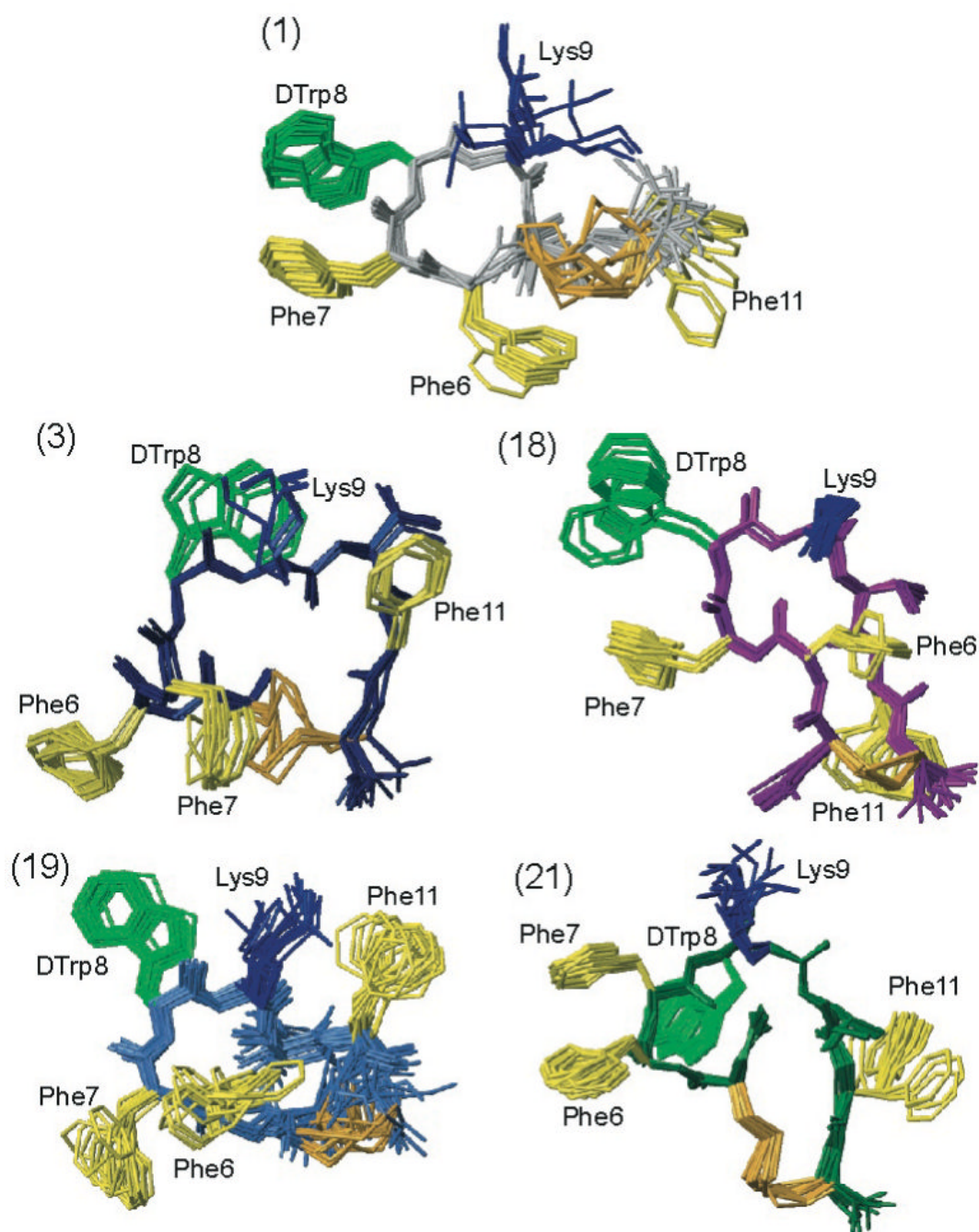


Figure 2.

The NMR structures of the five analogues studied by NMR (i.e., analogues **1**, **3**, **18**, **19** and **21** as indicated). For each analogue, twenty energy-minimized conformers with the lowest target function are used to represent the 3D NMR structure. The bundle is obtained by overlapping the C^α atoms of all the residues. The backbone and the side chains are displayed including the disulfide bridge. The following color code is used: grey (**1**) H-c[Cys-Phe-Phe-^δTrp-Lys-Thr-Phe-Cys]-OH, ODT-8 taken from Grace *et al.*;³⁴ navy-blue (**3**)H-c[Cys-Phe-Phe-^δTrp-Lys-Thr-Phe-^δCys]-OH; violet (**18**) Ac-c[^δNcy-Phe-Phe-^δTrp-Lys-Thr-Phe-Ncy]-OH; royal blue (**19**) Ac-c[Ncy-Phe-Phe-^δTrp-Lys-Thr-Phe-Ncy]-OH; dark green (**21**) Ac-c [Hcy-Phe-Phe-^δTrp-Lys-Thr-Phe-Cys]-OH. The amino acid side chains which are proposed

to be involved in binding to the various SRIF receptors are highlighted: ϵ Trp at position 8 in light green, Lys at position 9 in blue, and Phe at positions 6, 7 and 11 yellow. The disulphide bridges are shown in orange for clarity.

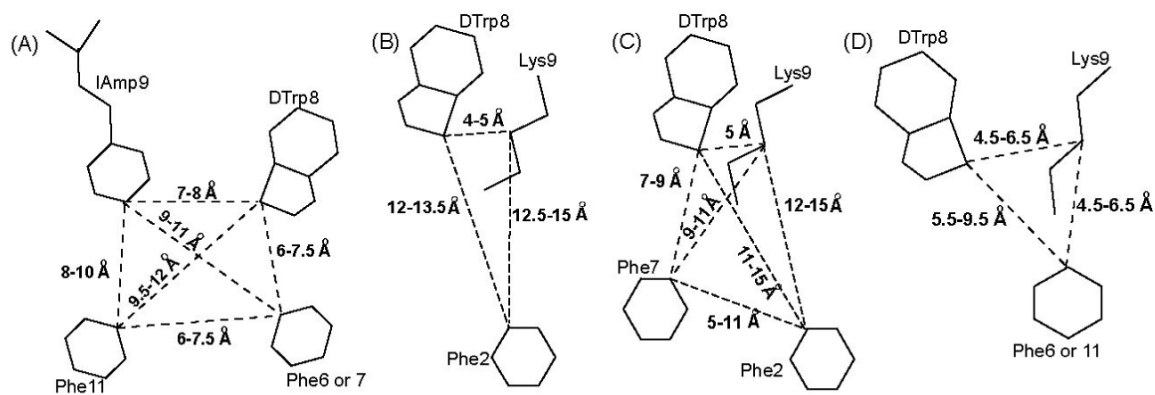


Figure 3.

Schematic drawings of agonist pharmacophores for receptor-selective analogues binding to the somatostatin receptors: (A) Sst₁, (B) Sst₂, (C) Sst_{2/5} and (D) Sst₄. The amino acid side chains, which are part of the pharmacophores and the distances between the corresponding C_γ atoms of the side chains are shown and are also listed in Table 3.

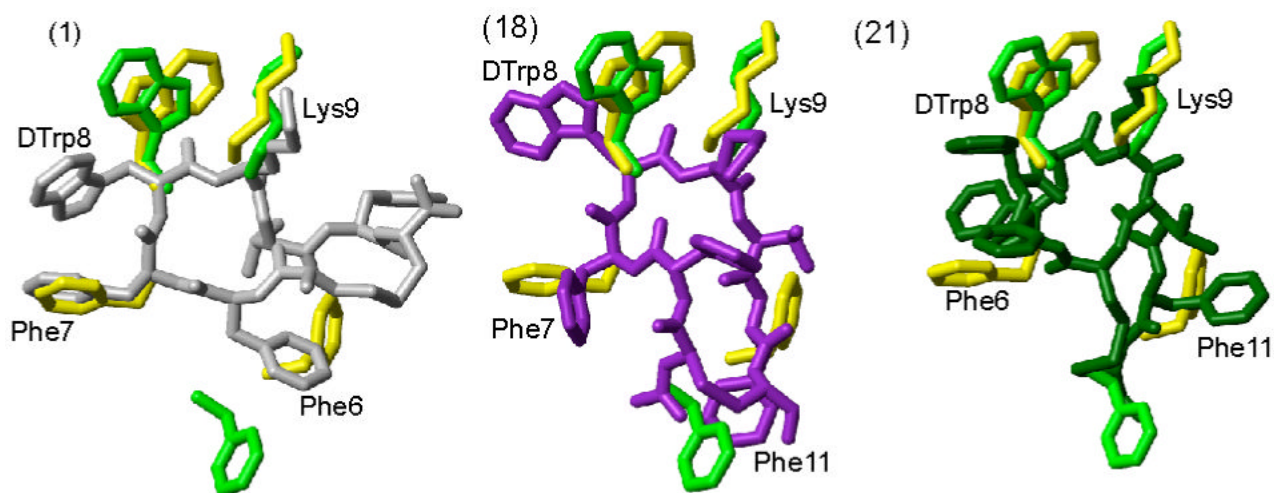


Figure 4. Superposition of receptor-specific pharmacophore with the 3D NMR structure of the analogues **1**, **18** and **21**. The sst_2 pharmacophore⁴¹ is shown in green. The octreotide pharmacophore proposed by Melacini *et al.*⁴⁴ is shown in yellow. In both the pharmacophores only the side chains of the amino acids are shown that are involved in binding to the receptor. For analogues **1**, **18** and **21**, the conformer with the lowest energy is used to represent the 3D structures. The analogues are color coded as in Figure 2. The side chains of the amino acids, which are proposed to be involved in receptor binding, are labeled. Phe⁶ in analogue **1**, Phe¹¹ in analogues **18** and **21** should undergo a change in their conformation to fit either the sst_2 or octreotide pharmacophores.

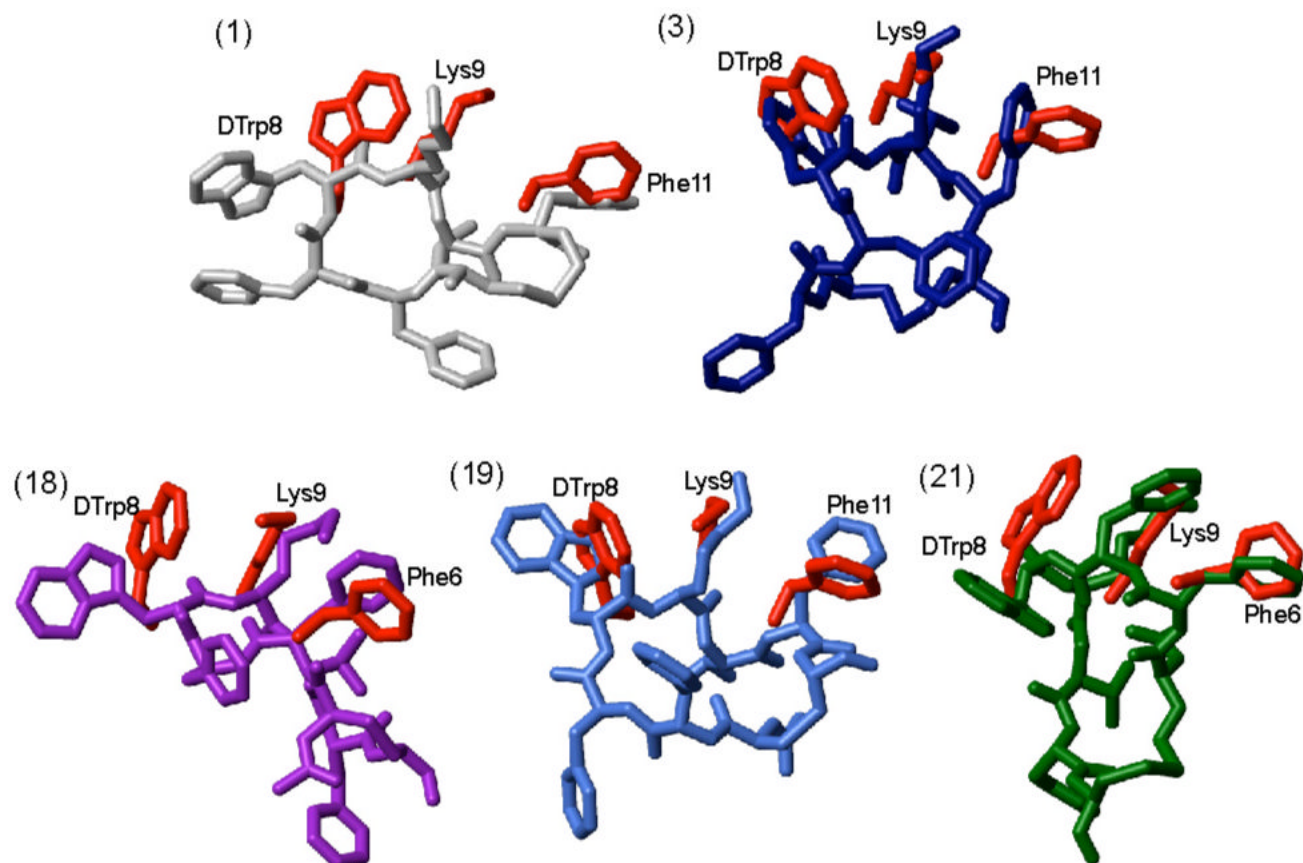


Figure 5. Superposition of sst₄ receptor-specific pharmacophore with the 3D NMR structures of the analogues **1**, **3**, **18**, **19** and **21**. The sst₄ pharmacophore³⁴ is represented by amino acid side chains colored in red. The conformer with the lowest energy represents the 3D structures of the analogues and they are color coded as in Figure 2. In addition, for each analogue the amino acid side chains proposed to be involved in receptor binding are labeled.

Table 1

Physico-chemical properties and sst₁₋₅ binding affinities (IC₅₀s, nM) of the analogues and control peptide ODT-8 (1)

ID#Compound	Purity	MS ^c		IC ₅₀ nM ^d					Number of atoms in the cycle	
		M _{calc}	M _{+H} _{obs}	ss1	ss2	ss3	ss4	ss5		
	HPLC ^e /CZE ^b									
1 * ODT-8 [H-c(Cys ³ -Phe ⁶ -Phe ⁷ -Trp ⁸ -Lys ⁹ -Thr ¹⁰ -Phe ¹¹ -Cys ¹⁴)-OH] (SRIF numbering)	99	3145.45	3146.46	3.2 ± 0.3 (16)	2.6 ± 0.3 (18)	3.8 ± 0.6 (16)	3.4 ± 0.3 (16)	3.2 ± 0.5 (16)	38	
95	98	1078.45	1078.90	27 ± 3.4 (4)	41 ± 8.7 (6)	13 ± 3.2 (4)	1.8 ± 0.7 (4)	46 ± 27 (3)	26	
2 [D-Cys ³]-ODT-8	99	1078.44	1079.48	14 (11; 17)	14.5 (15; 14)	4.5 (4.4; 4.6)	1.0 (1.2; 0.8)	9.5 (11; 7.9)	26	
3 * [D-Cys ¹⁴]-ODT-8	99	1078.44	1079.23	>1K (2)	18 (17; 19)	18.5 (20; 17)	8.2 (9; 7.3)	27 (29; 24)	26	
4 [D-Cys ³ , D-Cys ¹⁴]-ODT-8	99	1078.44	1079.36	>1K (2)	11 (9; 12)	6.3 (6; 6.6)	2.6 (2.8; 2.4)	8.7 (8.6; 8.8)	26	
5 Ac-ODT-8	99	1120.45	1121.29	22 ± 8.8 (3)	49 ± 9 (4)	7.1 ± 0.9 (3)	1.3 ± 0.2 (4)	2.6 ± 1.2 (3)	26	
6 [D-Cys ³]-Ac-ODT-8	99	1120.45	1121.23	16 (19; 13)	8.0 (6.4; 8.6)	19 (7.8; 30)	0.7 ± 0.1 (3)	9.1 (8.9; 9.3)	26	
7 [D-Cys ¹⁴]-Ac-ODT-8	99	1120.45	1121.26	>1000 (4)	4.9 (5.3; 4.4)	12 (5.5; 18)	4.5 (4.7; 4.3)	11 (12; 10)	26	
8 [D-Cys ³ , D-Cys ¹⁴]-Ac-ODT-8	99	1120.45	1121.43	>1000 (4)	9 (11; 7)	15 (11; 18)	3.25 (3.3; 3.2)	7.4 (6.2; 8.5)	26	
9 [Ncy ³]-Ac-ODT-8	97	1106.44	1107.20	79 (107; 50)	33 (39; 26)	6.0 (3.9; 8)	1.9 ± 0.6 (3)	9.0 (5.9; 12)	25	
10 [Ncy ³]-Ac-ODT-8	99	1106.44	1107.23	416 ± 126 (4)	42 ± 11 (5)	14 ± 2.6 (4)	3.1 ± 0.9 (5)	46 ± 16 (4)	25	
11 [Ncy ¹⁴]-Ac-ODT-8	99	1106.44	1107.18	358 (540; 175)	41 (36; 45)	20 (13; 26)	2.0 ± 0.5 (3)	50 (39; 61)	25	
12 [D-Ncy ¹⁴]-Ac-ODT-8	98	1106.44	1107.18	>1000 (4)	5.4 (3.6; 7.1)	53 (22; 83)	6.0 (8.1; 3.9)	82 (38; 126)	25	
13 [D-Cys ³ , Ncy ¹⁴]-Ac-ODT-8	97	1106.44	1107.48	540 ± 171 (3)	18.5 (18; 19)	30 (31; 29)	1.5 ± 0.5 (3)	51 (84; 18)	25	
14 [D-Cys ³ , D-Ncy ¹⁴]-Ac-ODT-8	99	1106.44	1107.48	>1000 (4)	4.8 (4.3; 5.3)	3.6 (4.5; 2.7)	3 ± 0.8 (3)	17 (2.5; 9.8)	25	
15 [Ncy ³ , D-Cys ¹⁴]-Ac-ODT-8	99	1106.44	1107.44	>1000 (4)	11 (9; 13)	69 (21; 117)	4.4 (5.1; 3.6)	50 (15; 85)	25	
16 [D-Ncy ³ , D-Cys ¹⁴]-Ac-ODT-8	97	1106.44	1107.45	>1000 (5)	13 ± 2.7 (5)	28 ± 6.1 (4)	5.0 ± 0.6 (4)	50 ± 7.9 (3)	25	
17 [Ncy ³ , D-Ncy ¹⁴]-Ac-ODT-8	97	1092.42	1093.39	>1000 (4)	3.9 (6.2; 1.3)	50 (84; 16)	2.6 ± 0.7 (3)	60 (9.3; 26)	24	
18 [D-Ncy ³ , Ncy ¹⁴]-Ac-ODT-8	96	1092.42	1093.58	>1000 (2)	109 ± 8.5 (3)	45 (32; 58)	2.7 ± 0.3 (3)	107 (163; 51)	24	
19 * [Ncy ³ , Ncy ¹⁴]-Ac-ODT-8	99	1092.42	1093.37	302 (381; 222)	34 (32; 36)	19 (16; 22)	1.6 ± 0.2 (3)	57 (7.3; 40)	24	
20 [D-Ncy ³ , D-Ncy ¹⁴]-Ac-ODT-8	94	1092.42	1093.53	>1000 (4)	13 ± 2.5 (3)	31 (23; 38)	2.2 ± 0.6 (3)	21 (29; 12)	24	
21 * [Hcy ³]-Ac-ODT-8	97	1134.47	1135.88	96 (103; 89)	6.5 (6.1; 6.9)	38 (59; 17)	0.9 (0.61; 1.1)	28 (17; 38)	27	
22 [DHcy ³]-Ac-ODT-8	98	1134.47	1135.64	218 (306; 130)	40 (48; 32)	69 (74; 63)	1.4 (1.3; 1.5)	90 (57; 122)	27	

* 3D NMR structures of these analogues are presented in this paper.

^a Percent purity determined by HPLC using buffer system: A = TEAP (pH 2.5) and B = 60% CH₃CN/40% A with a gradient slope of 1% B/min, at flow rate of 0.2 mL/min on a Vydac C18 column (0.21 × 15 cm, 5-μm particle size, 300 Å pore size). Detection at 214 nm.

^b Capillary zone electrophoresis (CZE) was done using a Beckman P/ACE System 2050 controlled by an IBM Personal System/2 Model 50Z and using a ChromJet integrator. Field strength of 15 kV at 30 °C, mobile phase: 100 mM sodium phosphate (85:15, H₂O:CH₃CN) pH 2.50, on a Supelco PL75 capillary (363 μm OD × 75 μm ID × 50 cm length). Detection at 214 nm.

^c The calculated m/z of the monoisotope compared with the observed [M + H]⁺ monoisotopic mass.

^d The IC₅₀ values (nM) were derived from competitive radioligand displacement assays reflecting the affinities of the analogues for the cloned somatostatin receptors using the non-selective [¹²⁵I]-[Leu⁸, D-Trp²², Tyr²⁵]-SRIF-28, as the radioligand. Mean value ± SEM when N ≥ 3 (shown in parenthesis). In the other cases, mean is shown with single values in parenthesis.

Table 2
Characterization of the NMR structures of the analogues studied by NMR

ID#	NOE distance restraints	Angle restraints***	CYANA Target function**	Backbone RMSD (Å)	Overall RMSD (Å)	CFF91 energies (Kcal/mol)			Residual restraint violations on			
						Total energy	Van der Waals	Electrostatic	Distances		Dihedral Angles	
									No. ≥ 0.1 Å	Max (Å)	No. ≥ 1.5 deg	Max (deg)
1	116	22	0.001	0.65 \pm 0.12	1.39 \pm 0.21	192.7 \pm 18	100.5 \pm 3	30.2 \pm 2	0.1 \pm 0.1	0.04 \pm 0.03	0 \pm 0	0 \pm 0
3	163	18	0.08	0.18 \pm 0.09	0.62 \pm 0.12	214.3 \pm 4	142.7 \pm 2	71.6 \pm 3	0.9 \pm 0.1	0.12 \pm 0.04	0 \pm 0	0 \pm 0
18	110	16	0.08	0.13 \pm 0.04	0.72 \pm 0.15	178.2 \pm 2	132.5 \pm 2	45.7 \pm 1	0.8 \pm 0.0	0.09 \pm 0.00	0.9 \pm 0	0.9 \pm 0.04
19	88	24	0.11	0.72 \pm 0.20	1.12 \pm 0.15	185.5 \pm 6	137.2 \pm 6	48.3 \pm 8	1.0 \pm 0.2	0.15 \pm 0.06	0.5 \pm 0.5	0.4 \pm 0.4
21	111	29	0.015	0.17 \pm 0.07	0.79 \pm 0.21	193.2 \pm 4	143.8 \pm 2	49.5 \pm 2	0.3 \pm 0.1	0.50 \pm 0.07	0 \pm 0	0 \pm 0.04

* The bundle of 20 conformers with the lowest residual target function was used to represent the NMR structures of each analogue.

** The target function is zero only if all the experimental distance and torsion angle constraints are fulfilled and all non-bonded atom pairs satisfy a check for the absence of steric overlap. The target function is proportional to the sum of the square of the difference between calculated distance and isolated constraint or van der Waals restraints and similarly isolated angular restraints are included in the target function. For the exact definition see reference.

42

*** Meaningful NOE distance restraints may include intra-residual and sequential NOEs.⁴²

Table 3
Distances between C_γ atoms (in Å) of selected residues for the analogues studied by NMR and the selective sst-pharmacophores

Analyte	F ⁶ -F ⁷	F ⁶ -D ^W ⁸	F ⁶ -K ⁹	F ⁶ -F ¹¹	F ⁷ -D ^W ⁸	F ⁷ -K ⁹	F ⁷ -F ¹¹	D ^W ⁸ -K ⁹	D ^W ⁸ -F ¹¹	K ⁹ -F ¹¹
1	7.2-8.0	10.0-10.2	7.9-9.6	7.6-9.7	4.7-4.9	9.3-10.8	11.8-14.5	7.4-8.9	11.7-13.7	5.9-10.6
3	7.6-7.7	8.4-8.6	11.0-11.7	13.2-13.6	8.0-8.1	5.6-6.5	7.1-8.2	5.7-5.9	8.9-9.4	5.0-5.2
18	8.6-8.6	10.0-10.1	5.4-5.5	8.4-8.9	5.5-5.5	9.4-9.4	8.7-9.9	7.5-7.5	12.0-13.0	11.5-11.6
19	5.1-7.5	7.8-8.6	5.3-7.1	6.6-10.2	7.3-8.2	9.1-10.3	12.6-13.4	5.9-6.2	8.9-10.7	4.4-6.0
21	4.8-5.1	8.7-8.9	7.3-8.0	12.6-13.8	6.4-6.4	5.5-5.7	11.9-13.7	7.0-7.1	6.6-9.5	10.1-10.5
sst ₁ pharmacophore	-	-	-	-	6.0-7.5	9.0-11.0	6.0-7.5	7.0-8.0	9.5-12.0	8.0-10.0
sst ₄ pharmacophore	-	5.5-9.5	4.5-6.5	-	-	-	-	4.5-6.5	5.5-9.5	4.5-6.5
sst ₂ pharmacophore	-	F ² -D ^W ⁸	F ² -K ⁹	-	-	-	-	-	-	-
octreotide pharmacophore	5.0-11.0	11.0-15.0	12.0-15.0	-	7.0-9.0	9.0-11.0	-	5.0-5.0	-	-